An Investigation of Poly(thienylene vinylene) in Organic Photovoltaic Devices

Adam P. Smith,† Rachel R. Smith,‡ Barney E. Taylor,‡ and Michael F. Durstock*,†

Air Force Research Laboratory, Materials and Manufacturing Directorate, Wright-Patterson Air Force Base, Ohio, and University of Dayton Research Institute, Dayton, Ohio

Received April 1, 2004. Revised Manuscript Received August 10, 2004

The soluble, conjugated regioregular polymer poly(3-dodecyl-2,5-thienylene vinylene), PDDTV, was synthesized and blended with 1-(3-methoxycarbonyl)propyl-1-phenyl-[6,6]-C_{61}, PCBM, into bulk heterojunction photovoltaic devices, working toward the goal of being able to tune the spectral response. External quantum efficiency measurements detected a maximum response at 580 nm (coincident with the PDDTV absorption λ_{max}), which corresponds to approximately a 100 nm red-shift as compared to devices made from common MDMO-PPV:PCBM blends. A near linear relationship between the current and light intensity was observed for PDDTV:PCBM devices, with slight deviation at relatively high intensities. Surface topography was investigated by AFM to explore the relationship between the roughness of the film and the device efficiency. The best device performance was observed in a 1:10 PDDTV:PCBM weight ratio and had a power conversion efficiency of 0.24% under AM 1.5G solar illumination conditions. This performance is strongly dependent on the active layer thickness, the thin film morphology, and the PCBM concentration in the film. Further optimization of these conditions is expected to yield PDDTV:PCBM blend devices with significantly improved device performance.

Introduction

The search for inexpensive renewable energy sources has sparked considerable interest in the development of photovoltaics based on conjugated polymers and organic molecules.[1−3] While so-called "plastic" solar cells are not yet commercially viable because they have significantly lower power conversion efficiencies than their inorganic counterparts, the potential for low-cost fabrication of large area devices makes them attractive alternatives to both silicon photovoltaics and nonrenewable resources in general.

Of particular interest has been the exploration of bulk heterojunctions,[4,5] which exploit an ultrafast photoinduced charge-transfer reaction[6] from an electron-donating material to an electron-accepting one. Commonly used electron donors are conjugated polymers such as poly(phenylene vinylene) and polythiophene derivatives, while common acceptors are other conjugated polymers[7] or functionalized C_{60} derivatives (i.e., 1-(3-methoxycarbonyl)propyl-1-phenyl-[6,6]-C_{61}, PCBM). An intimate mixture of the materials provides an interpenetrating network of two phases with a large donor:acceptor (D:A) interfacial area. In this way, more efficient charge separation (and consequently device efficiency) is achieved by allowing more of the excitons to be harvested. This bulk heterojunction device concept has allowed for a significant improvement in efficiencies over previously employed polymer-based bilayer devices.[8] Indeed, power conversion efficiencies on the order of 3.5% under air mass (AM) 1.5 solar conditions have been reported for P3HT:PCBM[9] as well as for MDMO-PPV:PCBM blend systems[10] (P3HT = poly(3-hexylthiophene), MDMO-PPV = poly[2-methoxy-5-(3′,7′-dimethyloctyloxy)]-*p*-phenylene vinylene). Methods for further improvement of D:A device performance involve increasing the charge transport capability of the component materials, understanding and controlling the nanoscale morphology of the film, and broadening the spectral response of the active materials.

A challenge in conjugated polymer systems is that not only do they absorb within a narrow region of the solar spectrum, but also presently utilized substituted polythiophenes and poly(phenylene vinylenes) with band gaps on the order of 2.0−2.2 eV and maximum absor-

* Corresponding author. E-mail: michael.durstock@wpafb.af.mil.
† Air Force Research Laboratory.
‡ University of Dayton Research Institute.

(1) Halls, J. J. M.; Friend, R. H. In *Clean Electricity from Photovoltaics*; Archer, M. D., Hill, R., Eds.; Series on Photoconversion of Energy; Imperial College Press: River Edge, NJ, 2001; Vol 1, pp 377−445.
(2) Gregg, B. A. *J. Phys. Chem. B* **2003**, *107*, 4688.
(3) Brabec, C. J.; Padinger, F.; Sariciftci, N. S.; Hummelen, J. C. *J. Appl. Phys.* **1999**, *85*, 6866.
(4) Yu, G.; Gao, J.; Hummelen, J. C.; Wudl, F.; Heeger, A. J. *Science* **1995**, *270*, 1789.
(5) Shaheen, S. E.; Brabec, C. J.; Sariciftci, N. S.; Padinger, F.; Fromherz, T.; Hummelen, J. C. *Appl. Phys. Lett.* **2001**, *78*, 841.
(6) Sariciftci, N. S.; Smilowitz, L.; Heeger, A. J.; Wudl, F. *Science* **1992**, *258*, 1474.
(7) Halls, J. J. M.; Walsh, C. A.; Greenham, N. C.; Marseglia, E. A.; Friend, R. H.; Moratti, S. C.; Holmes, A. B. *Nature* **1995**, *376*, 498.
(8) Sariciftci, N. S.; Baun, D.; Zhang, C.; Srdanov, V. I.; Heeger, A. J.; Stucky, G.; Wudl, F. *Appl. Phys. Lett.* **1993**, *62*, 585.
(9) Padinger, F.; Rittberger, R. S.; Sariciftci, N. S. *Adv. Funct. Mater.* **2003**, *13*, 85.
(10) Brabec, C. J.; Shaheen, S. E.; Winder, C.; Sariciftci, N. S.; Denk, P. *Appl. Phys. Lett.* **2002**, *80*, 1288.

10.1021/cm049447n CCC: $27.50
Published on Web 10/16/2004

bances of around 2.3−2.5 eV do not overlap with the maximum solar photon flux (~1.8 eV).[11] Alternatively, alkyl-substituted poly(2,5-thienylene vinylenes) with band gaps in the range E_g = 1.6−1.8 eV (absorption maxima ~1.9−2.1 eV)[12,13] allow for an improved overlap of the polymer absorption spectrum with the solar emission. In addition, regioregular poly(thienylene vinylene)s have a relatively high degree of intermolecular ordering, which may improve film morphology and lead to an enhancement in the charge transport capability of the device thereby improving its performance. Recent work by Henckens et al.[14] on related poly(thienylene vinylene) materials has shown some initial promise for their potential use in photovoltaic devices. These studies utilized a sulfinyl precursor route, which required heat treatment of the films in order to convert the precursor polymer into its conjugated form. In this study, we present an investigation of bulk heterojunction organic devices fabricated with regioregular poly(3-dodecyl-2,5-thienylene vinylene) and PCBM blends as a first step toward being able to manipulate and broaden the overall spectral response of the device through the creation of multicomponent blend systems.

Experimental Section

Materials and Methods. The polymer poly(3-dodecyl-2,5-thienylene vinylene), PDDTV, was synthesized according to the procedure of Loewe and McCullough.[13] The batch utilized in this study had the following characterization information: determined via gel permeation chromotograpy (GPC), M_w = 29 650, M_n = 10 510, PDI = 2.82; UV−vis, $\lambda_{max}(CHCl_3)$ = 570 nm. PCBM was synthesized according to the procedure of Hummelen et al.[15] UV−vis absorption spectra were recorded with a Varian Cary 5000 UV−vis−NIR spectrophotometer. Polymer molecular weights were determined by GPC in THF (25 °C; flow rate 1.0 mL/min) relative to polystyrene standards using an Agilent 1100 series system equipped with a vacuum degasser, photodiode array and fluorescence detectors with a Polymer Labs 5-μm "mixed-C" GPC column, and a Wyatt Technology Corporation Optilab refractive index detector along with accompanying Wyatt Astra software.

Device Fabrication and Testing. Glass slides patterned with ITO (Donnelly Applied Films, Inc.) were cleaned by sonication sequentially in detergent, water, acetone, and methanol, followed by treatment in a low-power air plasma for several minutes with a Harrick PDC-32G plasma cleaner/sterilizer. The ITO-coated slides were spin coated with an aqueous solution of poly(ethylene dioxythiophene) doped with polystyrene sulfonic acid, PEDOT:PSS (Bayer AG). The resulting thin layer (~60−90 nm) was dried in a vacuum oven at 80 °C for 12−16 h then plasma treated for 20 s. Chlorobenzene solutions (~2% w/w) of the active components were spun-cast on the PEDOT:PSS-coated slides to give film thicknesses ranging from 20 to 180 nm by changing solution concentrations or spin speeds. Thermal evaporation and a shadow mask were used to deposit the Al top electrode (~100 nm) resulting in 10 distinct cells each with an active area of 0.165 cm^2. Preliminary testing of each of the 10 pixels was performed to select the most promising pixel prior to solar simulated analysis. The preliminary tests were: resistance measurements, short-circuit current (I_{sc}), open-circuit voltage (V_{oc}), and dark and illuminated current−voltage ($I-V$) while using a blue LED (λ_{max} ~475 nm) for illumination. The best performing pixel then underwent V_{oc}, I_{sc}, and dark and illuminated $I-V$ studies using an Oriel 300 W solar simulator with appropriate filters to provide AM 1.5G (100 mW/cm^2). The dark $I-V$ was used to determine the rectification ratio. The fill-factor (*FF*) was determined from the illuminated $I-V$ and is the maximum power delivered divided by the product of V_{oc} and I_{sc}. External quantum efficiency (EQE) studies were performed using a tungsten source on an Acton Spectra Pro 275 monochromator with order sorting filters. The probe beam was chopped at 21 Hz and the signal was detected with an EG&G PAR 5210 lock-in amplifier. Intensity dependence of the short-circuit current was performed by using metallized neutral density filters sequentially inserted into the light from a tungsten source to vary the intensity over 4 orders of magnitude. Atomic force micrographs (height contrast images) were recorded with a Digital Instruments Dimension 3100 atomic force microscope in tapping mode using silicon tips.

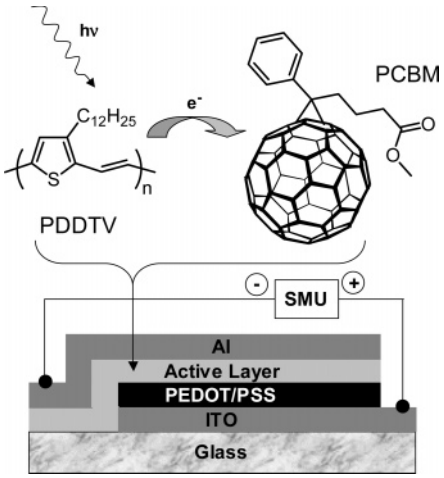

Figure 1. Photovoltaic device architecture and chemical structures of the active components.

Results and Discussion

Regioregular (>90% by ^{1}H NMR) poly(3-dodecyl-2,5-thienylene vinylene), hereafter referred to as PDDTV (see chemical structure in Figure 1), was synthesized by Stille cross-coupling of 2,5-dibromothiophene with (*E*)-1,2-bis(tributylstannyl)ethylene. While it is atypical that AA and BB type monomers would generate a regioregular polymer, the nature of the Stille mechanism may account for the experimentally observed structural regularity of PDDTV. Oxidative addition could preferentially occur at the less sterically hindered 5 position to generate a vinyl stannane AB-type *dimer*, which then couples with itself to generate the polymer.[13]

Bulk heterojunction cells with the sandwich structure ITO/PEDOT:PSS/X/Al, as shown in Figure 1, were fabricated where X was either pristine material or the polymer blended with PCBM in weight ratios varying from 1:1 to 1:20 (PDDTV to PCBM). A thin (<90 nm) PEDOT:PSS layer was used to provide a more uniform contact, to improve hole injection, and to eliminate shorts.[16,17] Devices consisting of a blended PDDTV:PCBM active layer exhibited V_{oc} and I_{sc} values that are

(11) Winder, C.; Matt, G.; Hummelen, J. C.; Janssen, R. A. J.; Sariciftci, N. S.; Brabec, C. J. *Thin Solid Films* **2002**, *403−404*, 373.
(12) Eckhardt, H.; Shacklette, L. W.; Jen, K. Y.; Elsenbaumer, R. L. *J. Chem. Phys.* **1989**, *91*, 1303.
(13) Loewe, R. S.; McCullough, R. D. *Chem. Mater.* **2000**, *12*, 3214.
(14) Henckens, A.; Knipper, M.; Polec, I.; Manca, J.; Lutsen, L.; Vanderzande, D. *Thin Solid Films* **2004**, *451-452*, 572.
(15) Hummelen, J. C.; Knight, B. W.; LePeq, F.; Wudl, F. *J. Org. Chem.* **1995**, *60*, 532.
(16) Zhang, F. L.; Gadisa, A.; Inganas, O.; Svensson, M.; Andersson, M. R. *Appl. Phys. Lett.* **2004**, *84*, 3906.
(17) Elschner, A.; Bruder, F.; Heuer, H.-W.; Jonas, F.; Karbach, A.; Kirchmeyer, S.; Thurm, S.; Wehrmann, R. *Synth. Met.* **2000**, *111−112*, 139.

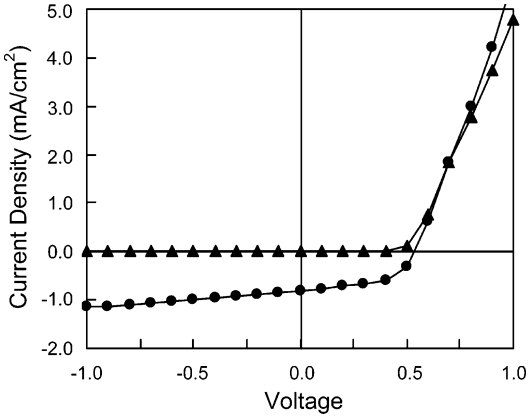

Figure 2. Current−voltage characteristics for an ITO/PEDOT:PSS/PDDTV:PCBM (1:10)/Al device in the dark (▲) and under illumination (●).

orders of magnitude higher than devices made from pristine PDDTV. Representative $I-V$ measurements are shown in Figure 2 for a PDDTV:PCBM (1:10) device. The dark $I-V$ curve displays a very low current under reverse bias and has a rectification ratio of 2000 at ± 1 V. Upon illumination under AM 1.5G conditions, the device exhibits an open-circuit voltage of 0.54 V and a short-circuit current density of 0.8 mA/cm^2. In comparison, devices made with a pristine PDDTV active layer show little to no rectification and have V_{oc} and I_{sc} values of 0.27 V and 2.2 × 10^{-3} mA/cm^2, respectively, upon illumination. The improved performance is likely the result of a photoinduced charge-transfer operating mechanism, whereby, upon excitation of the PDDTV and formation of an exciton, an ultrafast electron transfer to the C_{60} derivative occurs, resulting in the formation of separated charges which are then transported and collected at the electrodes.[6] While photoluminescence quenching is often indicative of this charge-transfer mechanism for many D:A blends,[6] this measurement is not feasible for poly(thienylene vinylene)s as they are inherently nonluminescent because an optical transition from the lowest energy excited state ($2A_g$) to the ground state ($1A_g$) is forbidden.[18,19] However, recent photoinduced absorption measurements confirm that charge transfer does occur from oligo(thienylene vinylene) analogues (2−12 repeat units) to the C_{60} derivative *N*-methylfulleropyrrolidine.[20] In addition, due to the large increase in performance observed between pristine PDDTV devices and those made with PDDTV:PCBM blends, it is believed that a charge transfer reaction is occurring in these devices. Light-induced electron spin resonance (LESR) measurements are currently underway to confirm the presence of polymer and PCBM radicals in films under illumination.[21]

The external quantum efficiency (EQE) spectrum for a PDDTV:PCBM (1:6) device, as shown in Figure 3a, exhibits a peak at 580 nm as well as a smaller one at

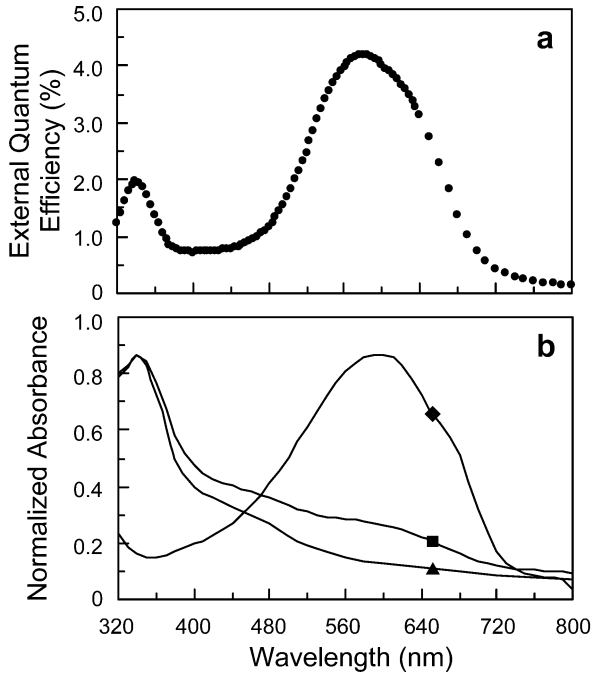

Figure 3. (a) External quantum efficiency (EQE) of an ITO/PEDOT:PSS/PDDTV:PCBM (1:6)/Al device and (b) absorption spectra of PDDTV (◆), PCBM (▲), and a 1:6 wt % PDDTV:PCBM blend (■).

340 nm. Figure 3b shows the absorption spectrum of this device, as well as that of the individual, pristine components. The absorption spectrum of the blend appears to be a simple linear superposition of the component absorption spectra, suggesting that there is no ground-state interaction between the two. In addition, the peaks in the EQE spectrum are coincident with those in the absorption of the individual components. It should be noted that the peak due to the PDDTV at 580 nm is shifted by 100 nm to longer wavelength as compared to devices made with PPV derivatives[5,22] due to the lower band gap of poly(thienylene vinylene)s.

Interestingly, the relative contribution of the PDDTV (580 nm) over the PCBM (340 nm) is much greater in the EQE spectrum than in the absorbance spectrum of the blend. This suggests that while fewer photons are being absorbed by the PDDTV as compared to the PCBM ($A_{580} < A_{340}$ in the blend), those absorbed by the PDDTV contribute much more to the device performance. While it is presently unclear why this is the case, it is likely due in part to the onset of absorption from ITO and the glass substrate in this regime (<350 nm), but could also be the result of thin film interference.[23] Indications of this phenomenon have been observed in other devices and we are currently investigating it in more depth.

To determine the optimum active layer thickness for blended devices, a systematic study was performed whereby a 1:4 w/w PDDTV:PCBM solution in chlorobenzene was used to make a series of devices with thicknesses ranging from 20 to 180 nm by changing either solution concentration or the rate of spin coating.

(18) Brassett, A. J.; Colaneri, N. F.; Bradley, D. D. C.; Lawrence, R. A.; Friend, R. H.; Murata, H.; Tokito, S.; Tsutsui, T.; Saito, S. *Phys. Rev. B* **1990**, *41*, 10586.
(19) Lies, M.; Jeglinski, S.; Lane, P. A.; Vardeny, Z. V. *Synth. Met.* **1997**, *84*, 891.
(20) Apperloo, J. J.; Martineau, C.; van Hal, P. A.; Roncali, J.; Janssen, R. A. J. *J. Phys. Chem. A* **2002**, *106*, 21.
(21) Parisi, J.; Dyakonov, V.; Pientka, M.; Riedel, I.; Deibel, C.; Brabec, C. J.; Sariciftci, N. S. *Z. Naturforsch.* **2002**, *57a*, 995.
(22) Kroon, J. M.; Wienk, M. M.; Vernees, W. J. H.; Hummelen, J. C. *Thin Solid Films* **2002**, *403−404*, 223.
(23) Hoppe, H.; Arnold, N.; Sariciftci, N. S.; Meissner, D. *Sol. Energy Mater. Sol. Cells* **2003**, *80*, 105 and references therein.

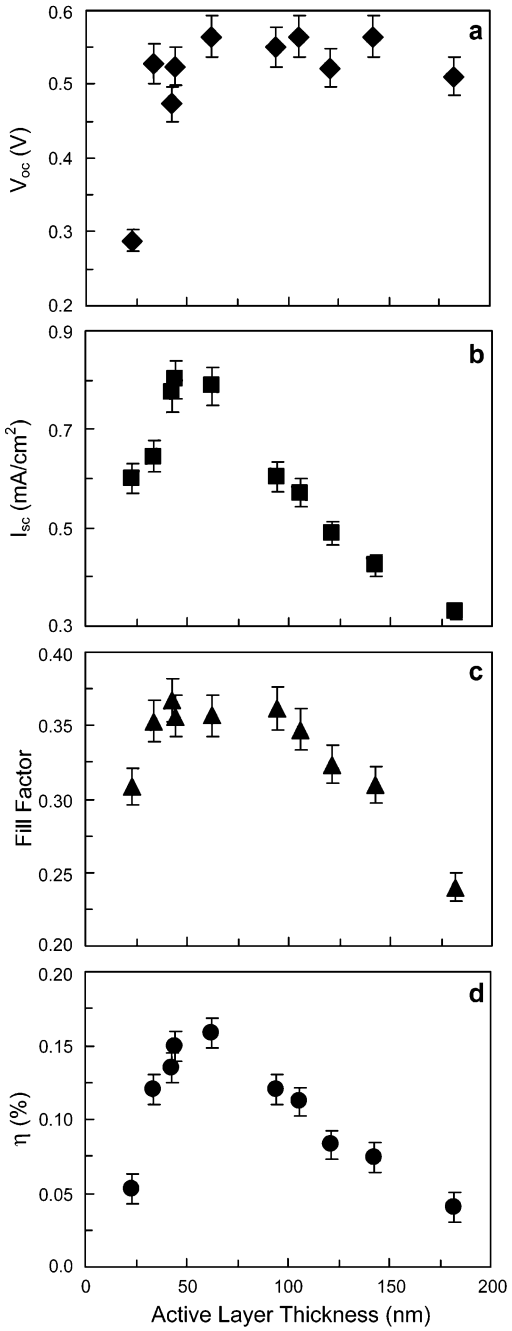

Figure 4. (a) V_{oc}, (b) I_{sc}, (c) *FF*, and (d) η dependence on active layer thickness for ITO/PEDOT:PSS/PDDTV:PCBM (1:4)/Al devices.

This D:A ratio was selected because a 1:3−1:4 range has conventionally been used for similar MDMO−PPV:PCBM bulk heterojunction devices.[5] Similarly, this thickness range was chosen because the optimal active layer thickness for a 1:3 or 1:4 wt % MDMO−PPV:PCBM blend has been reported to be ∼50−100 nm.[9,24] The PEDOT:PSS layers were ∼60 nm thick for all devices in this series. V_{oc}, I_{sc}, *FF*, and the power conversion efficiency (η) results under simulated solar illumination (AM 1.5G) are plotted versus film thickness in Figure 4. Open-circuit voltages were comparable (∼0.55 V) regardless of film thickness, with the exception of the 20 nm film, which had a V_{oc} of 0.29 V. This radical drop in potential could be due to local shorts in the device caused by pinholes in the active layer or similar film nonuniformities. This general trend in V_{oc} is consistent with other polymer:fullerene devices that also exhibit relatively constant open-circuit voltages.[25,26]

A maximum short-circuit current density of 0.8 mA/cm^2 and power conversion efficiency of 0.16% were measured for this system (where η is the maximum output electrical power divided by the incident optical power (100 mW/cm^2) at AM 1.5G). Both I_{sc} and η exhibit the best performance at around 50 nm, but values decrease for both thinner and thicker films. For very thin films, increasing the thickness results in an increase in the absorbance, resulting in more photons being harvested and an increase in the current. However, eventually, charge transport becomes a competing factor due to the low charge carrier mobility present in these materials. For relatively thick films, the charge carriers are unable to be transported through the film to the electrodes before recombination occurs, and this results in the observed decrease in current. It is believed that this is the same effect as seen in devices made from blends of MDMO−PPV and PCBM.[27,28]

The fill factor decreases as the active layer thickness is increased above 100 nm owing to the increased bulk series resistance component, $R_{s,\ bulk}$.[29] Below 100 nm, the *FF* remains relatively constant with the exception of the thinnest film, which, as discussed above, is likely due to film nonuniformity issues and the formation of pinhole defects.

The relative concentrations of the two component species can also play a major role in determining device performance. A 1:3−1:4 w/w D:A ratio is routinely employed for MDMO−PPV:PCBM bulk heterojunction devices. This proportion is approximately equivalent to one PCBM molecule for each polymer repeat unit (a 1:1 molar ratio). Since the molecular weight of the PDDTV repeat unit (276 g/mol) is comparable to that for MDMO−PPV (288 g/mol), one might expect the same PDDTV:PCBM weight ratio to provide the most efficient devices. Our investigation of devices with varying weight ratios of PDDTV and PCBM revealed that this was not the case. The V_{oc}, I_{sc}, *FF*, and η dependences on weight percent of PCBM are shown in Figure 5. To eliminate effects due to variations in thickness, all active layers were on the order of ∼50 nm, while PEDOT:PSS layers for this series were 70−90 nm. The open-circuit voltage for all concentrations, with the exception of pristine PDDTV, centers around 0.55 V. This result is also consistent with other polymer:fullerene systems where D:A ratios were modulated and relatively constant V_{oc} values were observed.[30] There are

(24) Fromherz, T.; Padinger, F.; Gebeyehu, D.; Brabec, C.; Hummelen, J. C.; Sariciftci, N. S. *Sol. Energy Mater. Sol. Cells* **2000**, *63*, 61.

(25) Mihailetchi, V. D.; Blom, P. W. M.; Hummelen, J. C.; Rispens, M. T. *J. Appl. Phys.* **2003**, *94*, 6849 and references therein.

(26) Brabec, C. J.; Cravino, A.; Meissner, D.; Sariciftci, N. S.; Rispens, M. T.; Sanchez, L.; Hummelen, J. C.; Fromherz, T. *Thin Solid Films* **2002**, *403*, 368.

(27) Halls, J. J. M.; Pichler, K.; Friend, R. H.; Moratti, S. C.; Holmes, A. B. *Appl. Phys. Lett.* **1996**, *68*, 3120.

(28) Nogueira, A. F.; Montanari, I.; Nelson, J.; Durrant, J. R.; Winder, C.; Sariciftci, N. S.; Brabec, C. J. *J. Phys. Chem. B* **2003**, *107*, 1567.

(29) The R_s, bulk component of the series resistance, was estimated by fitting the points about $I = 0$ to a linear regression. See Aernouts, T.; Geens, W.; Poortmans, J.; Heremans, P.; Borghs, S.; Mertens, R. *Thin Solid Films* **2002**, *403-404*, 297.

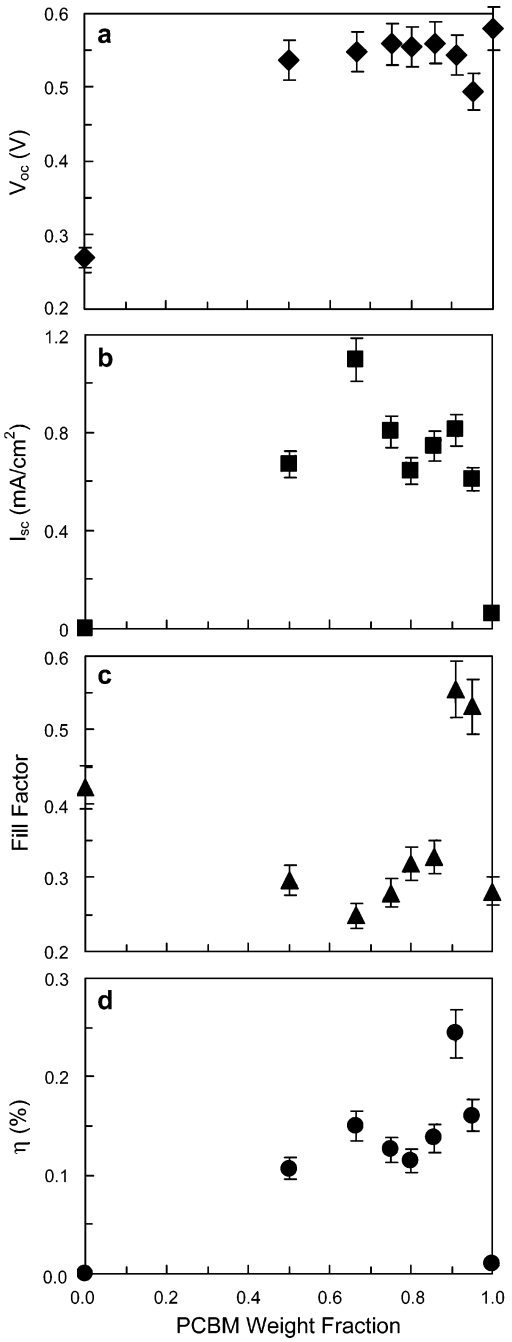

Figure 5. (a) V_{oc}, (b) I_{sc}, (c) *FF*, and (d) η dependence on PCBM weight fraction for ITO/PEDOT:PSS/PDDTV:PCBM/Al devices.

two peaks in both the I_{sc} and η plots occurring at 1:2 and 1:10 w/w (67% and 95% PCBM, respectively) while the *FF* centers around 0.30 for each blend device except for the 1:10 and 1:20 cells, where the fill factor nearly doubles.

To gain better insight into what might be controlling the individual parameters, atomic force microscopy (AFM) was used to examine the surface topography of the films. Figure 6 shows these height images, and their corresponding RMS roughness values (R_q), for the series of PDDTV:PCBM devices with varying compositions as discussed above. Films of pristine PDDTV and of PCBM (not shown) are smooth and featureless, and have a roughness of less than 1 nm. In contrast, the blended films exhibit a topography with apparently two distinct regions and with feature sizes and shapes that vary dramatically with composition. As the fraction of PCBM present in the film increases and the weight ratio goes from 1:1 to 1:4, the images clearly show features in which the surface tends to form "islands" which increase in size. In addition, the surface transitions from being very smooth with an R_q value of less than 1 nm for films of pristine PDDTV, to one that is quite rough with an R_q value of 20 and 18 nm for the 1:3 and 1:4 films, respectively. At a weight ratio of 1:4, the islands begin to coalesce. At even higher PCBM weight fractions (1:6), the continuous region of the surface has been reversed so that now the surface appears as a relatively smooth film with isolated concave depressions. At very high weight fractions of PCBM (1:10 and 1:20 weight ratios), a relatively smooth surface is again obtained with fewer of these depressions being observed.

It is important to note that the identity of these two distinct regions present in the surface topography of the films is not fully understood. It would appear that there is some degree of phase separation occurring such that two discrete phases are present in analogy to devices made from blends of MDMO−PPV and PCBM.[31−33] However, the relative composition of these phases is as yet uncertain, and their relative heights are drastically different as illustrated by the observed surface roughness. In fact, these roughness values are much larger than those observed for similar MDMO−PPV:PCBM devices (R_q = 1 nm).[5] In the most extreme cases of a 1:3 and a 1:4 weight ratio, these surface undulations become a significant portion of the total film thickness. Given the fact that the observed device efficiencies are significantly lower than those observed in the MDMO−PPV:PCBM devices, and the fact that our surface roughness values peak in the composition range where we expect maximum performance, it is believed that the depressed performance over this composition range occurs due to these very large fluctuations. Further improvement in performance will be obtained through a more thorough understanding of the dependence of film morphology upon processing conditions. Such efforts are currently underway.

The dependence of the short-circuit current density on light intensity was also examined for these devices and is summarized in Figure 7. Unlike previous measurements, which were performed under AM 1.5G solar illumination conditions, the intensity dependence of these devices was performed under illumination from a tungsten−halogen source, which is not matched to the solar spectrum. Despite this fact, the approximate intensity of 1 sun is shown on the graph. It should be realized, however, that this is only a rough approximation to give the reader an idea of the relative intensity

(30) Van Duren, J. K. J.; Yang, X.; Loos, J.; Bulle-Lieuwma, C. W. T.; Sieval, A. B.; Hummelen, J. C.; Janssen, R. A. J. *Adv. Funct. Mater.* **2004**, *14*, 425.

(31) Rispens, M. T.; Meetsma, A.; Rittberger, R.; Brabec, C. J.; Sariciftci, N. S.; Hummelen, J. C. *Chem. Commun.* **2003**, 2116.

(32) Gebeyehu, D.; Brabec, C. J.; Padinger, F.; Fromherz, T.; Hummelen, J. C.; Badt, D.; Schindler, H.; Sariciftci, N. S. *Synth. Met.* **2001**, *118*, 1.

(33) Martens, T.; D'Haen, J.; Munters, T.; Beelen, Z.; Goris, L.; Manca, J.; D'Olieslaeger, M.; Vanderzande, D.; De Schepper, L.; Andriessen, R. *Synth. Met.* **2003**, *138*, 243.

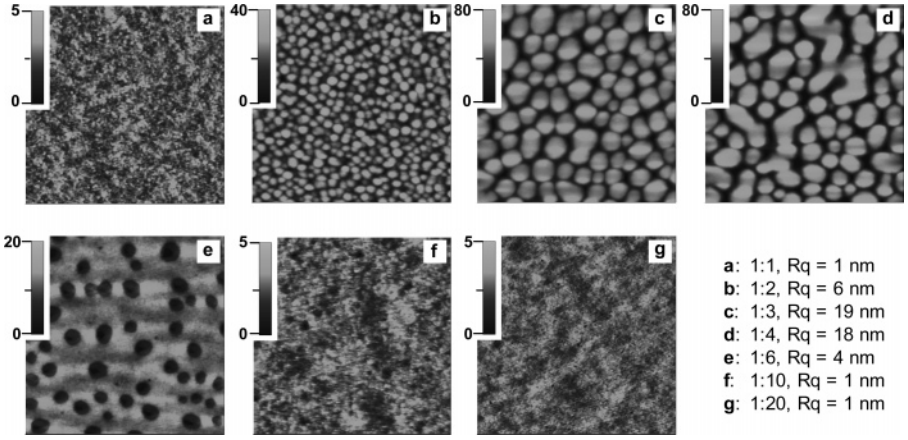

Figure 6. Tapping mode AFM height contrast images (2.5 μm × 2.5 μm) for PDDTV:PCBM blend devices. Z-scale bars are in units of nanometers.

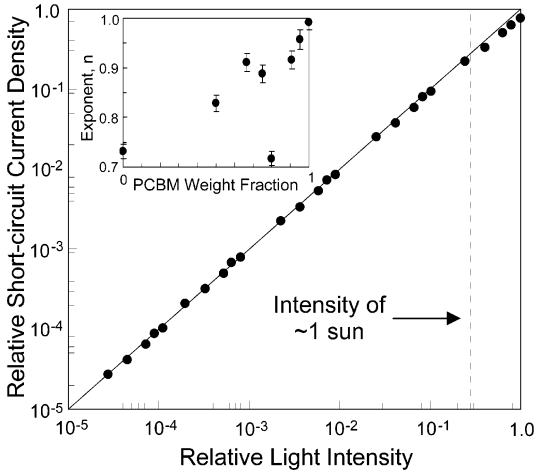

Figure 7. Current density as a function of relative intensity for a 1:10 PDDTV:PCBM device and (inset) exponent values from power fit of intensity data as a function of PCBM weight fraction.

and it should not be taken as rigorously correct due to the differing spectra. The log−log plot of current versus light intensity shows this relationship for a 1:10 PDDTV:PCBM device. The solid diagonal line in the figure illustrates a strictly linear relationship, and all of the devices followed this line at low intensities. However, sublinearity was observed at higher light intensities. To quantify the degree of sublinearity, the 10 most intense data points were fit via nonlinear least squares to a power law ($y = Ax^n$) whereby smaller values of the exponent, n, indicate a more sublinear relationship ($n = 1$ for a similar fitting of the lower intensity points). The exponent, n, in this power law fit to the data is shown versus PCBM weight percent in the inset of Figure 7. There appears to be a general trend in which the data become more linear with increasing PCBM concentration, with the exception of the 1:3 and 1:4 devices for which n was 0.89 and 0.72, respectively. The fact that this deviation occurs for films with the largest surface roughness values, as discussed above, further supports the notion that the large surface roughness leads to a decrease in the realizable device performance.

Conclusions

Photovoltaic devices fabricated with PDDTV:PCBM blend active layers exhibit a significant improvement in performance over pristine PDDTV films, thus supporting the occurrence of a photoinduced charge transfer reaction between the individual species. The best performing device was fabricated with a weight ratio of 1:10 (donor to acceptor) and exhibited a power conversion efficiency of 0.24%. The open-circuit voltage was relatively constant around 0.55 V, effectively independent of film thickness and composition, which is consistent with other polymer:fullerene devices. The short-circuit current and power conversion efficiency both exhibit a peak in their response at a film thickness near 50 nm due to the competing factors of increased optical absorption and bulk series resistance with increasing film thickness.

The composition of the blend film has a dramatic influence on both surface topography, as measured by AFM, and on device performance. Very large surface roughness values were observed in the composition range where maximum device performance was expected, suggesting a possible suppression in the realizable device efficiency. A more thorough understanding of the influence that processing conditions have on the film morphology is necessary to yield improved device performance.

Acknowledgment. We thank Dr. John B. Ferguson and Dr. John R. Reynolds for helpful discussions. The Office of Naval Research and the Air Force Office of Scientific Research are thanked for partial funding of this work.

CM049447N